Hard Scattering with Exclusive Reactions: $\pi^- p$ Elastic Scattering and ρ-Meson Production

G. C. Blazey, B. Baller, H. Courant, K. J. Heller, S. Heppelmann, M. L. Marshak, E. A. Peterson,
M. A. Shupe, and D. S. Wahl

University of Minnesota, Minneapolis, Minnesota 55455

D. S. Barton, G. M. Bunce, A. S. Carroll, and Y. I. Makdisi

Brookhaven National Laboratory, Upton, New York 11973

and

S. Gushue and J. J. Russell

Southeastern Massachusetts University, North Dartmouth, Massachusetts 02747

(Received 3 July 1985)

Initial results are presented from an experiment designed to test the dynamics of large-angle exclusive scattering. Cross sections are given for two reactions near 90° c.m., $\pi^- p \rightarrow \pi^- p$ (elastic) and $\pi^- p \rightarrow \rho^- p$, where $t = -8.9$ GeV$^2/c^2$ for 9.9-GeV/c incident pions. The ratio of $\rho^- p$/elastic is large, $\frac{2}{3}$, and remarkably similar to measurements for small-angle scattering.

Meson-baryon exclusive scattering at large momentum transfer has been proposed as a potentially rich laboratory for the study of hard-scattering processes.[1] If the characteristic scattering distance is much shorter than the hadron radius, it then seems reasonable to view these processes in terms of constituent interactions. Exclusive reactions at large t tend to probe the interaction of the valence quarks of the initial- and final-state wave functions, since, it is argued, any additional constituents would also have to be scattered to high t and this is improbable.[2] This picture is supported by the success of dimensional-counting arguments in the prediction of the energy dependence for both lepton and hadron elastic-scattering processes.[3] Thus, relationships can be expected to exist between different reactions according to the valence-quark wave functions of the particles involved; the helicities of all the quarks in the initial and final states are also determined by these wave functions.

This paper describes the first results from an experiment which was designed to test these ideas. The initial experiment studied $\pi^- p \rightarrow$ two-body final states for scattering near 90° in the center of mass. Examples are $\pi^- p \rightarrow \pi^- p, \rho^- p, K^0 \Lambda, K^+ \Sigma^-$. Cross sections for the first two reactions are presented; the analysis for the other final states is still in progress. These reactions differ in that either the final-state quarks are present in the initial state ($\pi^- p, \rho^- p$), new quarks have been created ($K\Lambda, K^+ \Sigma^-$), or, in addition, the quarks in the final-state baryon were part of the initial-state meson ($K^+ \Sigma^-$).

The simplest model for these reactions would argue that all quark-quark scattering amplitudes should be equal for scattering at 90°, and one would expect roughly equal cross sections for these reactions, in-

dependent of quark flavor.[4] Departures from this would imply dynamic effects at work. There are other models: One model uses perturbative QCD to determine the independent quark amplitudes[5]; a phenomenological model folds quark wave functions with summations over possible meson and baryon exchanges in the interactions.[6] These models make several clear and different predictions for ratios of cross sections and for final-state polarization.

A 9.9-GeV/c pion-beam momentum was chosen as a compromise between the desire to be as far into the high-energy regime as possible (the fixed-angle πp elastic-scattering cross section[7] shows an s^{-8} dependence, as expected from dimensional-counting arguments,[3] for pion momenta above 6 GeV/c), and yet obtain sufficient data in the face of the rapidly falling cross sections.

We report here cross sections for the exclusive reactions $\pi^- p \rightarrow \pi^- p$ and $\pi^- p \rightarrow \rho^- p$ at 90° in their center of mass. For elastic scattering at 90° and for our incident beam momentum of 9.9 GeV/c, $t = -8.9$ GeV$^2/c$ and the transverse momentum is $p_T = 2.1$ GeV/c. The absolute value of the incident momentum is known by various independent checks to within $\pm 1.5\%$. The experiment was performed in the C1 line at the Brookhaven Alternating-Gradient Synchrotron and the beam flux was typically 5×10^7 particles per pulse of the slowly extracted beam with a momentum spread of $\Delta p/p = \pm 1.5\%$ (rms). Finely segmented scintillator hodoscopes in the beam determined incident-particle position and angle at the liquid-hydrogen target.

A single-arm spectrometer (Fig. 1), set at 22° in the laboratory, detected the stable positively charged particle from the interaction (the proton in this case) and a
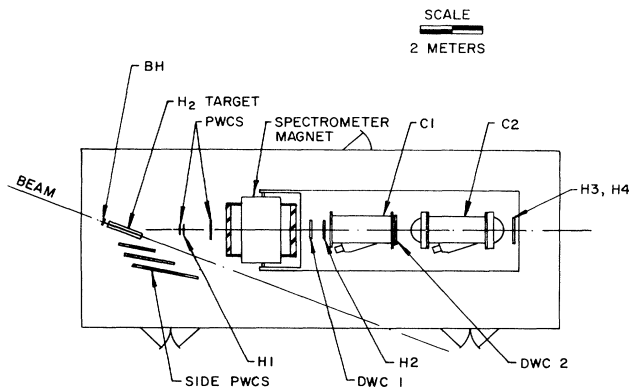
© 1985 The American Physical Society

FIG. 1. Plan view of the detector: BH and H1–H4 are scintillation-counter hodoscopes; PWC and DWC refer to proportional and drift wire chambers; and C1 and C2 are threshold gas Cherenkov counters for pions and kaons, respectively. The spectrometer magnet bent positive particles down and defined a narrow range of production angles about 22° in the laboratory.

large-aperture array of proportional wire chambers recorded track information on the opposite side. In the spectrometer arm a vertically deflecting magnet was placed so that its horizontal gap defined a range of laboratory angles, $\Delta\theta = \pm 2.5°$. The magnet bent positives down with a transverse kick of 0.8 GeV/c. Vertical deflection allowed us to make a momentum selection at the trigger level despite the large horizontal projection of the 1-m-long target. On the assumption of a point source in the vertical projection, a momentum could be determined by means of a matrix trigger between drift cells in DWC1 and DWC2 after the magnet. An event trigger was set for $\pi^- p \rightarrow$ positive $+ X$, with p_T within the limit set by the matrix (full acceptance above 1.9 GeV/c dropping to no acceptance below 1.4 GeV/c). Events were collected simultaneously for $\pi^- p$, $\rho^- p$, $K^+ \Sigma^-$, $\pi^+ \Delta^-$, and other exclusive final states which contain a stable positive particle. Two threshold Cherenkov counters were used to distinguish between pions, kaons, and protons in the spectrometer arm. The momentum resolution of the arm was $\Delta p/p = 0.5\%$.

5.4×10^6 events were recorded for 4.7×10^{12} incident pions on target. Most triggers were caused by the more copious lower momentum particles which either were accepted by the trigger or scattered from the magnet iron and fooled the trigger. 3% of the events on tape had a single spectrometer track with $p_T > 1.8$ GeV/c. Half the spectrometer tracks had no Cherenkov signal, which indicated a spectrometer proton. Of these, 23% had a single side track which formed an acceptable vertex with the incident beam track and the track in the spectrometer arm.

We show in Fig. 2(a) the missing-mass distribution for those events with a proton in the spectrometer and
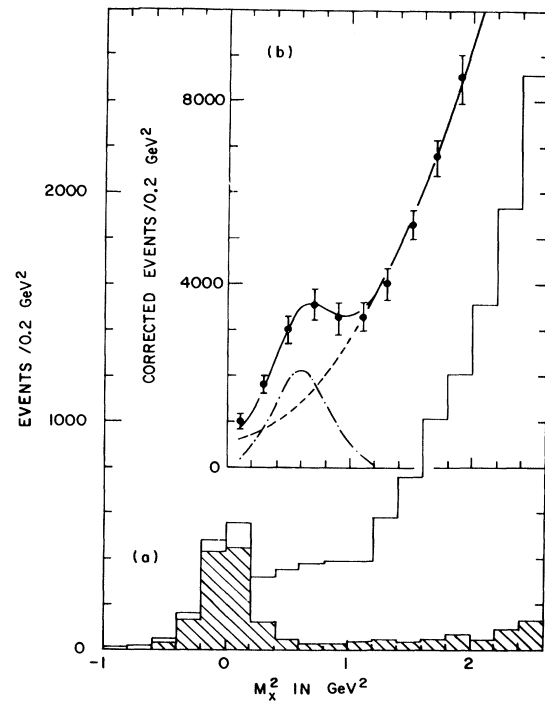

FIG. 2. (a) Event distribution in missing mass squared (M_X^2) for the reaction $\pi^- p \rightarrow p + X$. The shaded events are left after the requirement of elastic opening angle and coplanarity cuts. The shoulder which remains after the elastics are removed contains the candidate $\pi^- p \rightarrow \rho^- p$ events. (b) Geometric-acceptance–corrected event distribution in missing mass squared for the reaction $\pi^- p \rightarrow p + X$, after elastics and events with extra hits are removed. The dot-dashed line, a Gaussian, represents a resolution-smeared ρ and the dashed line is a fit to background. The fit is described in the text.

single track in the side array and an acceptable vertex. An elastic sample, the shaded region, was selected by our additionally requiring appropriate coplanarity and opening-angle cuts. There were approximately 1200 elastic events with an estimated $(7 \pm 2)\%$ background which were divided into center-of-mass angle bins of $\Delta \cos\theta^* = 0.02$.

After elastics are removed, candidate ρ events appear as a shoulder in the 0.6-GeV² region in Fig. 2(a), along with a large background contamination. This background presumably consists of nonresonant $\pi^- \pi^0$, three-pion events with only one track in the side array, and resolution-smeared events from higher missing mass. It was found that there were considerably more extra hits present for events at higher missing mass. We therefore chose to cut the nonelastic data on the extra-hit distribution in order to reduce the multipion background. However, the cut also eliminated a large fraction of good events which contained extra hits from "noise." The effect of the cut on the acceptance was monitored by its effect on the elastic

sample, where half the events were lost. The cut improved the ρ signal over background by a factor of 2 as determined from a fitting procedure described below. We also used the elastic data to check that the extra hits associated with the elastics were indeed randomly distributed over the chambers.

The missing-mass-squared (M_X^2) distribution with the acceptance corrected for the spectrometer arm (to remove trigger bias) and with elastics removed [Fig. 2(b)] was fitted by a form representing a resolution-smeared ρ resonance $(\sigma = 0.23$ GeV$^2)$ and a background. The background was characterized by a constant term and a quadratic term in M_X^2. This procedure gave 220 $\rho^- p$ events and parametrized the shape of the background, with a χ^2 per degree of freedom (DF) for the fit of 0.3. The ρ data were then divided into three bins with $\Delta \cos\theta^* = 0.08$ and this background shape was used to fit the data in the three $\cos\theta^*$ bins, with only the ratio of integrated signal to background varied. The fits for the individual bins were acceptable $(\chi^2/\text{DF} \approx 1)$, giving ratios of signal to all events in the missing-mass-squared region of 0.25 to 0.75 GeV^2 from 0.50 to 0.66. We have assigned errors on the background ratio of $\pm 15\%$ by comparing fit results for simulated data with various signal-to-background ratios and shapes.

Total incident beam was monitored to $\pm 20\%$ by a large-angle counter telescope which was calibrated at low intensity relative to a scintillation counter in the beam. Data runs with the target emptied gave a very low trigger rate and a negligible number of reconstructed events. Two differential Cherenkov counters were used to measure a pion fraction of 0.99 in the negative beam.

A Monte Carlo simulation was used to determine the acceptance of the apparatus. Elastic and $\pi^- p \rightarrow p\rho^-$ events were generated (the decay $\rho^- \rightarrow \pi^- \pi^0$ was generated with the observed decay distribution as described in the following paper) with multiple scattering included; the track information was coded as with real events, a simulated event trigger was applied, and events were reconstructed in the same way for the real and fake data. Chamber efficiencies, as measured from less constrained event triggers, were included in the simulation. Absorption and pion decay were small effects which were included in the cross-section calculation.

Figure 3 shows the measured differential cross sections for $\pi^- p \rightarrow \pi^- p$ (elastic) and $\rho^- p$ final states. The errors are dominated by statistics for the elastic data and by our estimate of the backgrounds for the $\rho^- p$ data. There is an overall $\pm 20\%$ systematic error from the beam-flux normalization which is not included in the errors shown. There were 1200 elastic events and 220 $\rho^- p$ events in the sample. (We note that the acceptance for the $\rho^- p$ events was approximately half
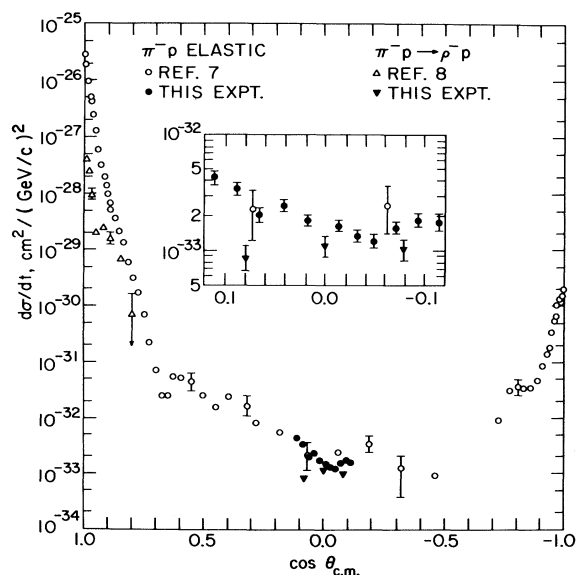

FIG. 3. The cross-section results for elastic and $\pi^- p \rightarrow \rho^- p$ reactions from this experiment are compared with other available data. A few representative error bars are shown. The area around 90° is shown in more detail in the inset.

the elastic acceptance. This difference is mainly due to the additional cut applied to the ρ data to improve the signal-to-background ratio.) Figure 3 also shows previous measurements of the elastic cross section[7] at 9.84 GeV/c and small-angle $\rho^- p$ data at 6 GeV/c.[8] We have scaled the 6-GeV/c data to 9.9 GeV/c by multiplying by the factor $6^2/9.9^2$.[9]

We find that the $\rho^- p$ cross section is nearly as large as the elastic at 90°. Although the elastic cross section has been measured previously at large angle and at our energy, the only previous $\rho^- p$ data are at forward angles. As can be seen in Fig. 3, the $\rho^- p$-to-elastic ratio is apparently similar in two very different kinematic regions: near 90° $(t = -8.9$ GeV$^2/c^2)$ where the cross sections are approximately flat in $\cos\theta^*$ and scale as s^{-8} for fixed θ^*, and for near-forward scattering $(t \sim -1$ GeV$^2/c^2)$ where the cross sections are falling rapidly and scale as s^{-2} at fixed t.

A phenomenological quark model which assumes that the scattering is mediated by a sum of meson exchanges is consistent with these 90° cross sections.[6] The naive statistical picture discussed in the introduction where it is assumed that all quark-quark amplitudes are of similar magnitude is also consistent with a large $\rho^- p$/elastic ratio,[4] but this model also demands that many other exclusive reactions be large.

The power of the use of exclusive reactions to pinpoint the dynamics of hard scattering lies in the measurement of a large number of different reactions. The present results do not yet restrict the mechanisms

for large-angle exclusive scattering, partly because perturbative QCD models do not yet calculate absolute cross sections. These models will be severely tested by the addition of results for other final states. For example, a perturbative QCD calculation predicts a factor of 16 difference in $\rho^- p/\rho^+ p$ according as quark exchange or quark annihilation dominates.[10] Data for other reactions have been taken with a π^- beam, e.g., $\pi^- p \rightarrow K^0\Lambda, K^+\Sigma^-, pA_2, \pi^+\Delta^-$, and for a tagged π^+ beam. These results will be presented in future publications. Other critical tests involve the final-state polarization of the ρ^-. In the following Letter we describe the analysis of the ρ^- decay distribution which tests helicity conservation in the perturbative QCD picture.

---

[1]P. Grannis, in Brookhaven National Laboratory Report No. BNL 50947, 1978 (unpublished).

[2]G. P. Lepage and S. J. Brodsky, Phys. Rev. D **22**, 2157 (1980).

[3]S. J. Brodsky and G. R. Farrar, Phys. Rev. D **11**, 1309 (1975).

[4]P. Fishbane and C. Quigg, Nucl. Phys. **B61**, 469 (1979).

[5]G. R. Farrar, Phys. Rev. Lett. **53**, 28 (1984).

[6]G. Nardulli, G. Preparata, and J. Soffer, Phys. Rev. D **31**, 626 (1985).

[7]D. P. Owen et al., Phys. Rev. **181**, 1794 (1969); K. A. Jenkins et al., Phys. Rev. Lett. **40**, 425 (1978); see C. Baglin et al., Nucl. Phys. **B216**, 1 (1983), for data at other energies. Small-angle elastic data are an average of 8.9- and 10.8-GeV/c data from K. J. Foley et al., Phys. Rev. Lett. **11**, 425 (1963).

[8]H. A. Gordon, K. W. Lai, and J. M. Scarr, Phys. Rev. D **8**, 779 (1973).

[9]This scaling procedure was checked by comparison of $\pi^- p \rightarrow \rho^0 n$ data at 6 (Ref. 8) and 17 GeV/c [G. Grayer et al., Nucl. Phys. **B75**, 189 (1974)].

[10]H. J. Lipkin, Phys. Rev. Lett. **53**, 2075 (1984).